

Effect of Protein Aggregation on the Binding of Lysozyme to Pyrene-Labeled Polyanions

Takeshi Sato,[†] Kevin W. Mattison,[‡] Paul L. Dubin,[‡] Mikiharu Kamachi,[†] and Yotaro Morishima^{*,†}

Department of Macromolecular Science, Graduate School of Science, Osaka University, Toyonaka, Osaka 560-0043, Japan, and Department of Chemistry, Indiana University-Purdue University, Indianapolis, Indiana 46202

Received April 2, 1998. In Final Form: July 9, 1998

The binding of lysozyme to pyrene (Py)-labeled homo- and copolymers of sodium 2-(acrylamido)-2-methylpropanesulfonate and acrylamide was investigated by a combination of scattering techniques (turbidimetry, quasielastic light scattering, and electrophoretic light scattering), potentiometry, and fluorescence techniques. Lysozyme, a basic protein with a high isoelectric point of 11.5, is known to exist in a dimer form at $\sim 5 < \text{pH} < \sim 10$ and in an aggregate form at $\text{pH} > \sim 10$. Potentiometric titration indicates binding of lysozyme aggregates to Py-labeled polysulfonates in 0.2 M NaCl at pH as high as 12.3. Nonradiative energy transfer (NRET) from tryptophan residues of lysozyme to Py labels commences near pH 10.5 when pH is further decreased. This onset of NRET is accompanied by an onset of solution turbidity, arising from the formation of lysozyme-polymer complexes with diameters 10–100 times larger than those of the individual components. This pH for the onset of NRET and turbidity, which is independent of both ionic strength and polymer linear charge density, is close to the pH at which the lysozyme aggregate dissociates into dimers. With a further decrease in pH, macroscopic phase separation occurs due to the association of the complexes of the lysozyme dimers with the polymer; the pH at which the macroscopic phase separation commences to occur is dependent on ionic strength.

Introduction

Interactions between polyelectrolytes and globular proteins can be found in many biological systems. The classical example is the synthesis of proteins in cellular systems, where every major step in the synthesis process (DNA transcription, RNA translation, and protein folding) is controlled by electrostatic and hydrophobic interactions between the macromolecular constituents.¹ Protein-polyelectrolyte interactions are also central to many industrial applications, examples of which are purification of proteins by selective precipitation or coacervation with polyelectrolytes,² polyelectrolyte modification of protein-substrate affinity,³ and immobilization and stabilization of enzymes in polyelectrolyte complexes.⁴

Kabanov et al.,^{4–7} Dubin et al.,^{8–14} and others^{15–18} have investigated protein-polyelectrolyte complexes (PPCs) by

sedimentation,^{6,7} turbidimetry,^{5–7,11–18} static light scattering,^{5,7,9,15} quasielastic light scattering (QELS),^{9,11,14,15} and electrophoretic light scattering (ELS).^{8,9,11,15} These techniques have proven to be powerful in obtaining information about the global structure of PPCs. For example, the existence of a “primary” soluble complex, composed of a number of proteins bound to a single polymer chain, has been revealed by means of these techniques.^{6–8,15} Li et al.⁹ used light scattering techniques to show that the binding of bovine serum albumin (BSA) with polycations occurred in a cooperative fashion. More recently, capillary electrophoresis has been used to quantify the binding of proteins to polyelectrolytes, yielding information on the average number of proteins bound and the cooperativity of the binding event.¹⁰

Dubin et al.^{13,19,20} found that the complex formation between polyelectrolytes and oppositely charged particles, such as proteins and charged micelles, exhibits a phase transition-like feature and can be described to a first approximation by

* Author to whom all correspondence should be sent.

[†] Osaka University.

[‡] Indiana University-Purdue University.

(1) Shaner, S. L.; Melancon, P.; Lee, K. S.; Burgess, R. R.; Record, M. T., Jr. *Cold Spring Harbor Symp. Quantum Biol.* **1983**, *47*, 463.

(2) Stregge, M. A.; Dubin, P. L.; West, J. S.; Flinta, C. D. In *Protein Purification: from Molecular Mechanisms to Large-Scale Processes*; Ladisch, M.; Willson, R. C.; Panton, C. C.; Builder, S. E., Eds.; American Chemical Society: Washington, DC, 1990; Chapter 5.

(3) Ruckpaul, K.; Rein, H.; Jänig, G. R.; Pfeil, W.; Ristau, O.; Damaschun, B.; Damaschun, H.; Müller, J. J.; Pürschel, H. V.; Bleke, J.; Scheler, W. *Stud. Biophys.* **1972**, *34*, 81.

(4) Kabanov, V. A. In *Macromolecular Complexes in Chemistry and Biology*; Dubin, P. L. et al., Eds.; Springer-Verlag: New York; 1994; p 151.

(5) Kabanov, V. A.; Zezin, A. B.; Mustafaev, M. I.; Kasaikin, V. A. In *Polymeric Amines and Ammonium Salts*; Goethals, E. J., Ed.; Pergamon: Oxford, 1980; p 173.

(6) Kabanov, V. A.; Evdakov, V. P.; Mustafaev, M. I.; Antipina, A. D. *Mol. Biol.* **1977**, *11*, 582.

(7) Zaitsev, V. S.; Izumrudov, V. A.; Zezin, A. B.; Kabanov, V. A. *Dokl. Phys. Chem. USSR* **1992**, *322*, 17.

(8) Xia, J.; Dubin, P. L.; Kim, Y.; Muhoherac, B. B.; Klimkowski, V. *J. Phys. Chem.* **1993**, *97*, 7, 4528.

(9) Li, Y.; Mattison, K. W.; Dubin, P. L.; Havel, H. A.; Edwards, S. L. *Biopolymers* **1996**, *38*, 527.

(10) Gao, J. Y.; Dubin, P. L.; Muhoherac, B. B. *Anal. Chem.* **1997**, *69*, 2945.

(11) Xia, J.; Dubin, P. L.; Morishima, Y.; Sato, T.; Muhoherac, B. B. *Biopolymers* **1995**, *35*, 411.

(12) Wen, Y-p.; Dubin, P. L. *Macromolecules* **1997**, *30*, 7856.

(13) Mattison, K. W.; Brittain, I. J.; Dubin, P. L. *Biotechnol. Prog.* **1995**, *11*, 1, 632.

(14) Park, J. M.; Muhoherac, B. B.; Dubin, P. L.; Xia, J. *Macromolecules* **1992**, *25*, 290.

(15) Tsuboi, A.; Izumi, T.; Hirata, M.; Xia, J.; Dubin, P. L.; Kokufuta, E. *Langmuir* **1996**, *12*, 2, 6295.

(16) Kokufuta, E.; Shimizu, H.; Nakamura, I. *Macromolecules* **1981**, *14*, 1178.

(17) Kokufuta, E.; Shimizu, H.; Nakamura, I. *Macromolecules* **1982**, *15*, 1618.

(18) Kokufuta, E.; Takahashi, K. *Polymer* **1990**, *31*, 1177.

(19) Dubin, P. L.; Rigsbee, D. R.; McQuigg, D. W. *J. Colloid Interface Sci.* **1985**, *105*, 509.

(20) Dubin, P. L.; Chew, C. H.; Gan, L. M. *J. Colloid Interface Sci.* **1988**, *128*, 566.

$$\xi\sigma_C \sim \mu^{1/2} \quad (1)$$

where ξ is the linear charge density of the polyelectrolyte, σ_C is the critical surface charge density of the charged particle at the critical conditions for incipient complex formation, and μ is the ionic strength of the solution. Because the Debye parameter κ is proportional to $\mu^{1/2}$, this dependence suggests that complex formation is governed by electrostatic interaction.

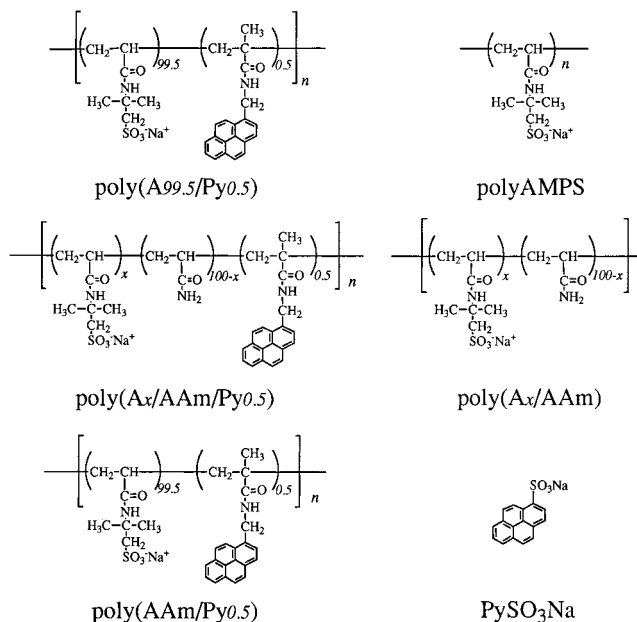
The methods just described are essentially equilibrium techniques that provided no information about dynamics and little insight into the short-range organization. Fluorescence spectroscopy, however, can yield such information, particularly when both the protein and the polyelectrolyte have fluorescent chromophores. Xia et al.¹¹ reported that nonradiative energy transfer (NRET) occurred from excited tryptophan (Trp) in egg white lysozyme to pyrene (Py) labeled on a polyanion. More recently, Kuragaki and Sisido²¹ observed highly efficient NRET from Trp units in an avidin tetramer to a Py-labeled substrate (biotin). Because most proteins have Trp residues and because the critical distance between Trp and Py for NRET can be comparable to the mean radius of many proteins, NRET techniques may be of use to obtain information about the microscopic structure of PPCs and the dynamics of complex formation. Potentiometric titration is an additional technique that can be used to examine PPC microstructure.^{12,13,18} In contrast to light scattering techniques, which are sensitive to the long-range (10–1000 nm) organization of the complex, potentiometric titrations are coupled to shorter-range phenomena and interactions, that is, changes in protein pK.

In the present work, we combine "macroscopic" techniques (turbidimetry, QELS, and ELS) with "microscopic" techniques (NRET and potentiometry) to investigate the binding of lysozyme with Py-labeled poly(sodium 2-(acrylamido)-2-methylpropanesulfonate-co-acrylamide) with varying compositions (see Scheme 1). Lysozyme, a basic protein composed of a large number of basic amino acid residues, has a very high isoelectric point (pI) of 11.5.²² It is known that lysozyme exists in its monomeric form in acidic aqueous solutions (pH < ~5) but forms dimers in the pH region from ~5 to 10, and aggregates at pH > ~10.^{23,24} Monomeric lysozyme is a relatively small protein with the approximate dimensions 3 × 3 × 4.5 nm²⁵ (much smaller than BSA), and it consists of a high portion of aromatic amino acid residues including six Trp residues, three of which are located near the cleft (Trp 62, 63, and 108).²² In this work, we attempted to clarify apparently complicated interactions of lysozyme aggregates and dimers with the polyelectrolytes by the techniques just described.

Experimental Section

Materials. *N*-(1-Pyrenylmethyl) methacrylamide was prepared as reported previously.²⁶ 2-(Acrylamido)-2-methylpropanesulfonic acid (AMPS) and acrylamide (AAm) were purchased from Wako Pure Chemical Company and were recrystallized from

Scheme 1



methanol and benzene, respectively. 2,2'-Azobis(isobutyronitrile) (AIBN), purchased from Nacalai Tesque Inc., was recrystallized from methanol prior to use. Sodium 1-pyrenesulfonate (PySO₃-Na) was purchased from Molecular Probes, Inc. and was used without further purification. Hen egg white lysozyme [EC3.2.1.17] was purchased from Sigma Chemical Company and was used as received.

Polymerization. Polymers (Scheme 1) were prepared by free-radical polymerization initiated with AIBN in *N,N*-dimethylformamide (DMF). In a typical procedure, a DMF solution of the monomers along with 0.5 mol % AIBN (on the basis of the total monomers), was deaerated by five freeze-pump-thaw cycles. Polymerization was carried out at 60 °C for 10 h. The polymer was precipitated with ether and purified by reprecipitation from methanol into excess ether three times. The polymer was then air-dried and dissolved in water. After neutralization of sulfonic groups with NaOH, the solution was dialyzed against pure water for 3 days. The polymer was recovered by lyophilization. Weight-average molecular weights (M_w) were determined from size-exclusion chromatography to be $(0.8-1.3) \times 10^5$ with a polydispersity $M_w/M_n \approx 2$.

Fluorometry. Fluorescence spectra were obtained at 25 °C using a Hitachi F-4500 spectrophotometer. A 0.2-mm cell, with the incident light angled at 45°, was used to minimize inner filter effects.²⁷ A lysozyme stock solution and a polymer stock solution of pH 12.0 were prepared separately. The ionic strengths were adjusted to predetermined values with NaCl. Each solution was filtered with an ADVANTECH 0.1- μ m syringe filter prior to use. Aliquots of the stock solutions were mixed to prepare sample solutions containing lysozyme (0.2 g/L) and the polymer (0.2 g/L).

To increase the number of net positive charges on the protein surface, pH was decreased by adding a 0.5 M HCl solution, dispensed from a Gilmont microburet. The solutions were stirred for 30 min to equilibrate before fluorescence measurements. Sample solutions at pH > 12 were prepared separately, taking into account the contribution of NaOH to the ionic strength because the concentration of NaOH (~0.1 M) was not negligible in this pH region.

For NRET experiments, the excitation wavelength was chosen as 290 nm. At this wavelength, absorbances for lysozyme (0.2 g/L) and poly(A99.5/Py0.5) (0.2 g/L) were 0.38 and 0.02, respectively. Hence, photons of the incident light were essentially absorbed by Trp residues in lysozyme; namely, Trp residues were excited selectively at this excitation wavelength. The fluorescence intensity (I) of Py labels was monitored at 376 nm.

(21) Kuragaki, M.; Sisido, M. *Bull. Chem. Soc. Jpn.* **1997**, *70*, 261.

(22) Imoto, T.; Johnson, L. N.; North, A. C. T.; Phillips, D. C.; Rupley, J. A. In *The Enzymes*, 3rd ed.; Boyer, P. D., Ed.; Academic: New York, 1972; Vol. 7, p 665.

(23) Sophianopoulos, A. J.; Van Holde, K. E. *J. Biol. Chem.* **1964**, *239*, 2516.

(24) Hampe, O. G.; Tondo, C. V.; Hasson-Voloch, A. *Biophys. J.* **1982**, *39*, 77.

(25) Blake, C. C. F.; Koenig, D. F.; Mair, G. A.; North, A. C. T.; Phillips, D. C.; Sarma, V. R. *Nature* **1965**, *206*, 757.

(26) Morishima, Y.; Tominaga, Y.; Kamachi, M.; Okada, T.; Hirata, Y.; Mataga, N. *J. Phys. Chem.* **1991**, *95*, 6027.

(27) Meech, S. R.; Philips, D. *J. Photochem.* **1983**, *23*, 193.

Turbidimetry. Turbidity measurements were conducted with the same samples as that for the fluorescence measurements with a Shimadzu UV-2500PC spectrophotometer using a 1-cm path length cell at 420 nm. All turbidity values are reported in the form 100-% transmittance (100-%*T*).

Potentiometry. The effect of the binding of polyelectrolyte on lysozyme amino acid p*K* values was determined using potentiometric titrations. Two 40-mL aliquots of a 0.6-g/L lysozyme solution, at pH 12.8 and ionic strength 0.2, were prepared by mass and purged with N₂. A 0.24-g sample of poly(A99.5/Py0.5) was added to one of the aliquot ([polymer] = 6.00 g/L), and both aliquots were titrated to pH 10 with 3.0 M HCl. In the two identical titrations, the initial pH (± 0.005) and initial mass (± 0.001 g) were constant. The Δ*H*⁺ versus pH plot was generated by subtraction of the polymer-free blank from the sample titration curve.

Electrophoretic Light Scattering (ELS). Electrophoretic mobilities for poly(A99.5/Py0.5), lysozyme, and their complex were measured at pH 12.0 at 25 °C using a DELSA 440 electrophoretic light scattering instrument (Coulter Instrument Company). The electric field was applied in constant-current mode, and the particle mobility at the stationary layer was measured at four scattering angles (8.6°, 17.1°, 25.6°, and 34.2°). The electrophoretic cell had a rectangular cross section (1 mm thick) connecting hemispherical cavities in each electrode, with a total cell volume of ~1 mL. The reported mobilities are an average of readings collected at different current values (range 0.5 to 12 mA).

Quasielastic Light Scattering (QELS). QELS measurements were carried out at 25 °C and at a scattering angle of 90° using an Otsuka Photal DLS-7000 light scattering system equipped with a 75 mW Ar⁺ laser (NEC) operating at a wavelength λ₀ = 488 nm in a vacuum. The autocorrelation decay curves were fitted with a multiexponential decay function using the Levenberg–Marquardt algorithm.^{28–30}

Results and Discussion

Fluorometric and Turbidimetric Titrations. Figure 1a shows a fluorescence spectrum for a lysozyme solution at pH 11.4, and fluorescence and absorption spectra for a poly(A99.5/Py0.5) solution at the same pH. The solutions were excited at 290 nm. From the spectral overlap between the lysozyme emission and Py absorption spectra, the Förster radii (*R*₀)^{31,32} for NRET from Trp in lysozyme to Py in the polymer were calculated to be 2.0 and 2.4 nm at pH 12.0 and 7.5, respectively. The *R*₀ value depends on pH because the fluorescence quantum yield of Trp residues in lysozyme depends on pH (e.g., the quantum yield at pH 7.5 is nearly three times higher than that at pH 12.0^{33,34}). These *R*₀ values are close to the dimension of lysozyme. Thus, Py labels can sense only lysozyme molecules bound to the polyanions at Py sites.

An example of a set of fluorescence spectra for a mixture of lysozyme (0.2 g/L) and poly(A99.5/Py0.5) (0.2 g/L) in 0.2 M NaCl solution at varying pHs (pH 8.0–12.8) is given in Figure 1b. The quantum yield of Trp fluorescence depends on the solution pH,^{33,34} so the fluorescence intensity at 340 nm, which is solely due to the Trp emission, increases as the pH is decreased. On the other hand, the intensity of Py fluorescence at 376 nm is independent of pH. Thus, any pH-dependent enhancement of the Py fluorescence intensity can be attributed to NRET from Trp to Py labels. Accordingly, we can discuss the energy transfer based only on the changes in the Py fluorescence

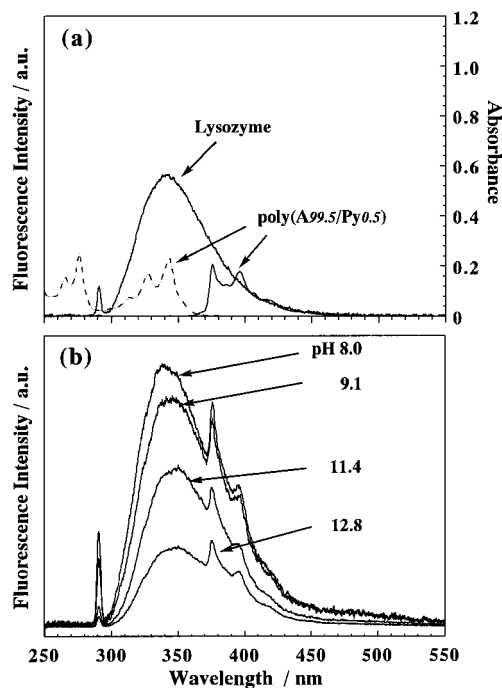


Figure 1. (a) Fluorescence spectra, excited at 290 nm, for 0.2 g/L lysozyme and 0.2 g/L poly(A99.5/Py0.5) in 0.2 M NaCl at pH 11.4. The Py absorption spectrum (broken line) is included for reference. (b) Fluorescence spectra, excited at 290 nm, for 0.2 g/L lysozyme with 0.2 g/L poly(A99.5/Py0.5) in 0.2 M NaCl at pH 12.8, 11.4, 9.1, and 8.0.

intensity. The Py fluorescence intensity cannot directly be determined in the lysozyme–poly(A99.5/Py0.5) system, because the Trp fluorescence spectrum overlaps the Py fluorescence spectrum, as seen in Figure 1a. However, because Trp is the sole contributor to the fluorescence intensity at 340 nm (Figure 1a), the contribution of Trp fluorescence intensity at any wavelength can be calculated from the measured intensity at 340 nm. Therefore, the Py fluorescence intensity at 376 nm (I_{Py}^{376}) can be obtained by correcting the measured value (I_{LP}^{376}) as follows:

$$I_{\text{Py}}^{376} = I_{\text{LP}}^{376} - \left(I_{\text{LP}}^{340} \frac{I_{\text{Lys}}^{376}}{I_{\text{Lys}}^{340}} \right) \quad (2)$$

where I_{LP}^{376} and I_{LP}^{340} are the fluorescence intensities for the lysozyme–poly(A99.5/Py0.5) system at 376 and 340 nm, respectively. The ratios $I_{\text{Lys}}^{376}/I_{\text{Lys}}^{340}$ were determined from the fluorescence spectra for free lysozyme solution at corresponding pH in 0.2 M NaCl, where I_{Lys}^{376} and I_{Lys}^{340} are the fluorescence intensities at 376 and 340 nm, respectively.

Relative intensities for Py fluorescence (I/I_0) for the lysozyme–poly(A99.5/Py0.5) system at varying ionic strengths (*μ*) are plotted against pH in Figure 2a. Here, *I* is the calculated Py fluorescence intensity (I_{Py}^{376}) at a given pH and *I*₀ is the Py fluorescence intensity in the absence of lysozyme. When the pH is decreased from 12.8, the *I/I*₀ ratio begins to increase near pH 10.5 regardless of the ionic strength. Turbidimetric titration data are shown in Figure 2b for comparison with the fluorescence data. There is a well-defined pH for the onset of turbidity (100-%*T*), which is also independent of the solution ionic strength. This pH coincides with the pH for the onset of NRET. The simultaneous occurrence of NRET and a turbidity increase is to be noted, especially because NRET can be considered as a microscopic phenomenon, whereas

(28) Eckert, A. R.; Webber, S. E. *Macromolecules* **1996**, *29*, 560.

(29) Levenberg, K. *Quart. Appl. Math.* **1944**, *2*, 164.

(30) Marquardt, D. W. *J. Soc. Indust. Appl. Math.* **1963**, *11*, 431.

(31) Birks, J. B. In *Photophysics of Aromatic Molecules*; Wiley-Interscience: New York, 1970; p 567.

(32) Oevering, H.; Verhoeven, J. W.; Paddon-Row, M. N.; Cotsaris, E.; Hush, N. S. *Chem. Phys. Lett.* **1988**, *143*, 488.

(33) Cowgill, R. W. *Arch. Biochem. Biophys.* **1963**, *100*, 36.

(34) Cowgill, R. W. *Biochim. Biophys. Acta* **1970**, *200*, 18.

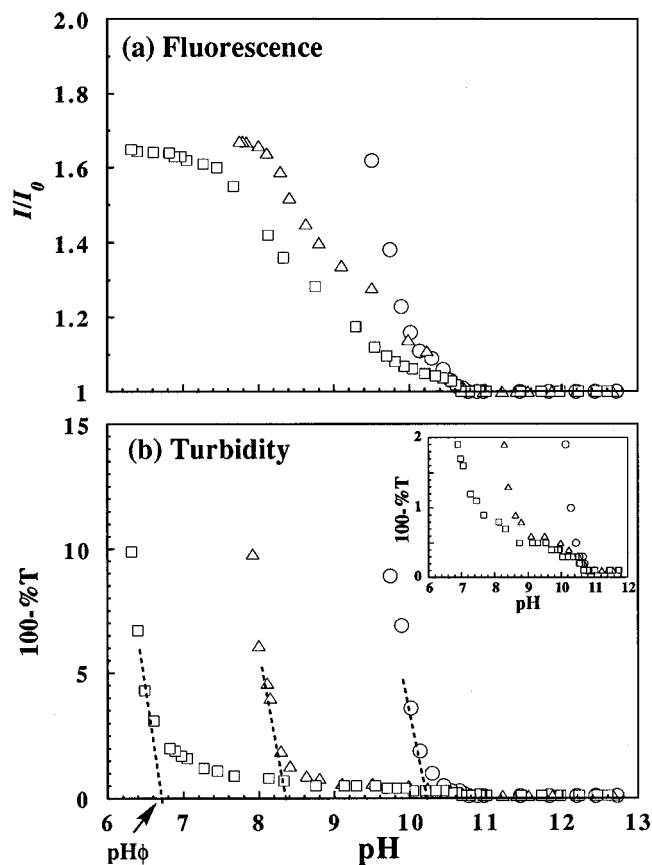


Figure 2. Fluorometric (a) and turbidimetric (b) titration data for the lysozyme–poly(A99.5/Py0.5) system: [lysozyme] = 0.2 g/L, [polymer] = 0.2 g/L. The ionic strengths are 0.1 (○), 0.2 (△), and 0.3 (□). I and I_0 are the fluorescence intensity for poly(A99.5/Py0.5) at a given pH and the intensity in the absence of lysozyme at pH 11.5, respectively. The excitation wavelength is 290 nm.

solution turbidity is generally considered to be macroscopic in nature, that is, the magnitude of NRET is dependent on the number of lysozyme–Py pairs that allow NRET and the distance between the donor and the acceptor, whereas the solution turbidity is dependent on the molecular weight of the complex and the number of complexes in the path length. We will come back to this point later. Figure 2b shows that the pH at which bulk phase separation occurs (pH_0), represented by a sharp increase in turbidity, is strongly dependent on ionic strength. These observations imply that the interaction between lysozyme and polyelectrolyte that leads to NRET is not governed by electrostatic interaction, whereas the bulk phase separation is controlled by electrostatic interaction.

The effect of the polymer linear charge density (ξ) on the lysozyme–polymer interaction using the Py-labeled copolymers of AMPS and AAm with varying AMPS contents (99.5, 70, and 50 mol %; Scheme 1) was also examined. The fluorometric and turbidimetric titration data are presented in Figure 3. Both I/I_0 and turbidity commence to increase near pH 10.5 regardless of the AMPS content in the copolymer upon decrease in solution pH starting from pH 12.8. These findings also imply that the phenomenon occurring near pH 10.5 is not governed by electrostatic interaction.

Another possible factor that could induce interaction between lysozyme and the Py-labeled polyelectrolyte is hydrophobic interaction (i.e., it may be possible that Py labels interact with a hydrophobic surface region of

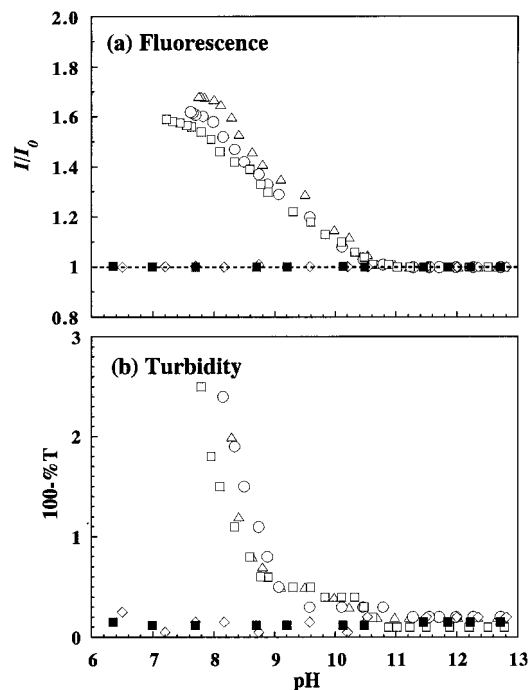


Figure 3. Fluorometric (a) and turbidimetric (b) titration data for 0.2 g/L lysozyme in the presence of poly(A99.5/Py0.5) (△), poly(A70/AAm/Py0.5) (○), poly(A50/AAm/Py0.5) (□), poly(AAm/Py0.5) (◇), and PySO_3Na (■) in 0.2 M NaCl. I and I_0 are the fluorescence intensity for poly(A99.5/Py0.5) at a given pH and the intensity in the absence of lysozyme at pH 11.5, respectively. The excitation wavelength is 290 nm.

lysozyme). Fluorometric and turbidimetric titration data for Py-labeled poly(acrylamide) [poly(AAm/Py0.5)] and sodium 1-pyrenesulfonate (PySO_3Na) are presented in Figure 3. As can be seen in this Figure, poly(AAm/Py0.5) does not induce complex formation, evidenced by no NRET in the whole pH range examined. In addition, the negatively charged PySO_3Na does not bind to lysozyme. These findings suggest that hydrophobic interaction between a small amount of hydrophobes (0.5 mol % Py) in the copolymers and lysozyme is insufficient to initiate complex formation and that the high electrostatic potential of polyelectrolytes is required for the complex formation.

There may be a possibility that hydrogen bonding between amide bonds in the polyanion and in lysozyme contributes to the PPC formation in interplay with electrostatic interactions. However, clarification on this possibility awaits future studies.

The absence of any effect of μ or ξ on the pH for the onset of NRET and turbidity is not consistent with electrostatic binding. On the other hand, the polyelectrolyte charge seems to be prerequisite for binding. Although electrostatic interaction is a predominant factor to induce the complexation, this apparent contradiction led us to consider the possibility that the fluorometric and turbidimetric titrations did not indicate the initial binding of lysozyme to the polyelectrolytes. Therefore, we investigated the initial binding using a potentiometric technique.

Potentiometric Titration. In previous studies we have shown that comparative potentiometric titrations can be used to monitor changes in protein pK values upon formation of protein–polyelectrolyte complexes.¹² In the present study this microscopic technique is complementary to the fluorometric and turbidimetric techniques because the influence of the charged polymer chain on protein pK values should be independent of both the location of the

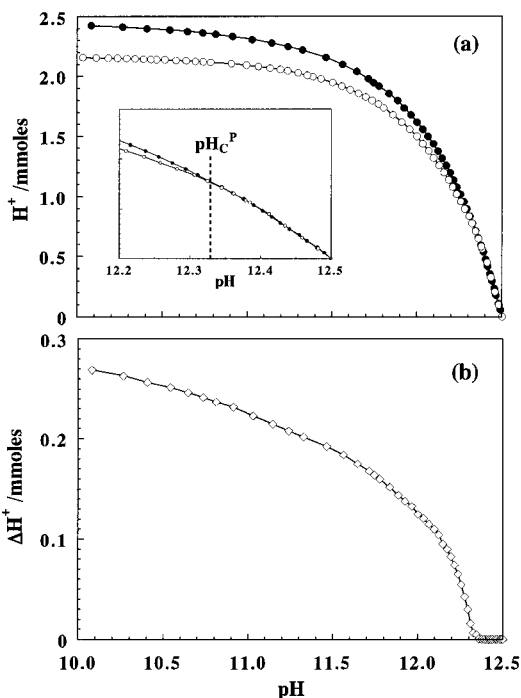


Figure 4. Potentiometric titration curves (a) for 40 mL solutions of 0.6 g/L lysozyme in the absence (○) and presence (●) of 6.0 g/L of poly(A99.5/Py0.5) in 0.2 M NaCl. Data converted from Figure 4a plotted as ΔH^+ (b).

pyrene probe and the molecular weight of the complex formed. Because in other protein–polyelectrolyte systems it has been shown that the critical pH at the critical conditions for incipient complex formation (pH_c) determined by this technique is independent of polyelectrolyte concentration,¹³ we increased both the polyanion and the protein concentrations in the potentiometric experiments for the sake of the sensitivity (i.e., the sensitivity of potentiometric titration technique depends on the concentration of bound protein and varies inversely with the ratio of free protein to bound protein.).

As observed in Figure 4a, the potentiometric titration curve for lysozyme in the presence of poly(A99.5/Py0.5) deviates from that of the lysozyme control solution, indicating that the binding of lysozyme to the polyelectrolyte increases the pK of the titratable residues (i.e., the polyanion-bound lysozyme is more basic). Figure 4b shows the difference in the amount of added H^+ (ΔH^+) plotted as a function of pH. The ΔH^+ value steeply increases at a well-defined pH (pH 12.3), indicating the binding of lysozyme to the polyanion.

Lysozyme can associate with polyanions by electrostatic interaction at pH 12.3, at which the net charge is negative, because positively charged residues (11 arginyl residues, whose pK_a value is 12.5³⁵) exist even at this pH. In fact, Park et al.¹⁴ reported that lysozyme interacted with polyAMPS above its pI (i.e., when the net charge of lysozyme was -2.6 ± 1) in 0.10 M NaCl. Therefore, we conclude that complex formation between lysozyme and the polyanion commences to occur at pH 12.3. Since the ΔH^+ value is indicative of the total number of bound proteins, the rapid increase in ΔH^+ at pH 12.3 suggests a phase transition-like behavior for the protein-binding phenomenon at $pH_c = 12.3$.

ELS. Although lysozyme binds to the Py-labeled polyelectrolyte at $pH < 12.3$, negligible NRET was

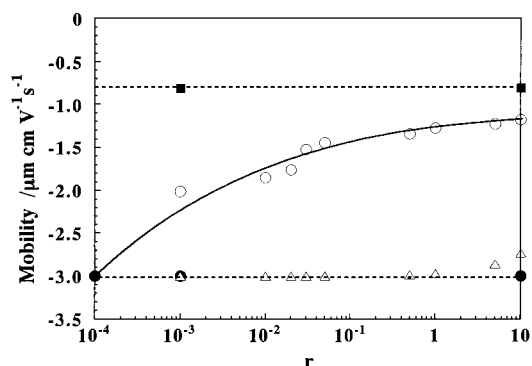


Figure 5. Electrophoretic mobility data for free lysozyme (■), free poly(A99.5/Py0.5) (●), and their complexes at varying r (= [lysozyme]/[polymer]) (○) at pH 12.0 in 0.2 M NaCl. The mobilities calculated from eq 3 for anti-cooperative binding (△) are included for reference.

observed in the pH region from 10.6 to 12.3. This result may be indicative of cooperative binding of lysozyme to the polyelectrolyte. If the binding is highly cooperative and independent of the Py label, there may be an insufficient number of Py–lysozyme complexes for NRET detection at low protein concentrations. Electrophoresis may be used to examine the type of binding in protein–polyelectrolyte systems.⁹ In the simplest case, the mobility (m) of a free draining soluble PPC is⁸

$$m = \frac{q_p + nq_{pr}}{f_p + nf_{pr}} \quad (3)$$

where q_p and q_{pr} are the charges for the polyelectrolyte and the protein, respectively, f_p and f_{pr} are the frictional coefficients for the polyelectrolyte and the protein, respectively, and n is the average number of bound proteins per PPC. For purely anti-cooperative binding, n is small at low protein concentration. Hence, the mobility of the PPC will be similar to that of the free polyelectrolyte. As the protein concentration is increased, n will also increase, resulting in a change in the soluble PPC mobility. As n becomes large, the complex mobility should approach that of the free protein. For purely cooperative binding, n is the same for all complexes and an increase in protein concentration influences only the concentration of PPC and not its mobility. Hence, the PPC mobility should be constant and similar to that of the free protein. Last, if the binding is noncooperative, the protein has no preference for any given type of binding site, and n is a statistical average taken across all of the polyelectrolytes.

The mobility data at pH 12.0 for free lysozyme, free poly(A99.5/Py0.5), and lysozyme–poly(A99.5/Py0.5) are shown in Figure 5. The mobilities calculated from eq 3 for purely anti-cooperative binding are included for reference. The mobility of the soluble PPC is not constant at low r (= [protein]/[polymer]), implying that the binding in the lysozyme–poly(A99.5/Py0.5) system is not highly cooperative, but the mobility behavior also differs substantially from that predicted for purely anti-cooperative binding. Finally, the high initial mobility at low r is inconsistent with noncooperative binding. The results indicate some degree of cooperativity in the present system. It can be concluded, however, that the binding of lysozyme to the Py-labeled polyanion without significant NRET is not a result of highly cooperative binding. Therefore, the lack of NRET at $pH > 10.5$ may relate to a systematic phenomenon resulting from negligible concentration of Trp residues within the Förster radius (~ 2.0 nm) for transfer from Trp to the Py label.

(35) Nozaki, Y. In *Tanpakushitsu no Kagaku* (in Japanese); Imahori, K.; Ui, N.; Narita, K.; Funatsu, M., Eds.; Tokyo Kagaku Doujin: Tokyo, 1976; Vol. 3, p 367.

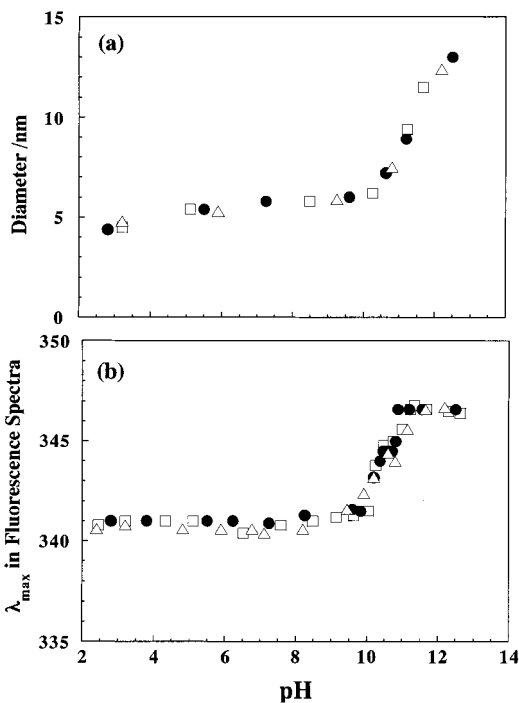


Figure 6. Apparent diameter (a) and λ_{\max} of Trp fluorescence (b) for 0.2 g/L lysozyme as a function of pH at varying ionic strengths: 0.1 (Δ), 0.2 (\bullet), and 0.3 (\square).

Aggregation of Lysozyme. We next focus on the self-associative behavior of lysozyme. It has been reported that lysozyme molecules exist as a "monomeric" form at $\text{pH} < \sim 5$ and they form aggregates above $\text{pH} \sim 10$.^{22,23} Between these two pHs, lysozyme exists in a dimer form.^{23,24} Figure 6a shows pH dependence of the apparent diameter of free lysozyme (0.2 g/L) measured by QELS at varying ionic strengths. The emission maximum (λ_{\max}) of lysozyme fluorescence is plotted as a function of pH in Figure 6b. The apparent diameters are ~ 6 nm in the pH region from 6 to 10, which may correspond to the lysozyme dimer.^{23,24} In a lower pH region (i.e., $\text{pH} < \sim 6$), the apparent diameter slightly decreases with a decrease in pH [i.e., the diameter decreases to ca. 4.5 nm near pH 3 (Figure 6a)], which may correspond to the monomeric form of lysozyme. In a higher pH region (i.e., $\text{pH} > \sim 10$), on the other hand, the diameter increases with an increase in pH, which is indicative of the aggregation of lysozyme. This increase in the apparent diameter at $\text{pH} > \sim 10$ is accompanied by a red shift of λ_{\max} , indicating that the Trp fluorescence is perturbed by aggregation. Thus, we may use the shift of λ_{\max} as an indication of the aggregation of lysozyme.

Another important observation in Figure 6 is that the changes in the diameter and in λ_{\max} are independent of ionic strength. Figure 7 shows λ_{\max} in the presence of poly(A x /AAm) (Scheme 1) with varying compositions (100, 70, and 50 mol % AMPS). In this experiment, we used the Py-free copolymers for simplicity of their fluorescence spectra of the lysozyme-polymer mixture. The aggregation of lysozyme is not affected by the presence of the polyanions regardless of their linear charge densities. Thus, it is possible that the lysozyme aggregation has an effect on NRET, the onset of which is independent of both ionic strength and the polymer linear charge density.

Because three out of six Trp residues near the hydrophobic active site of lysozyme (Trp 62, 63, and 108) exhibit

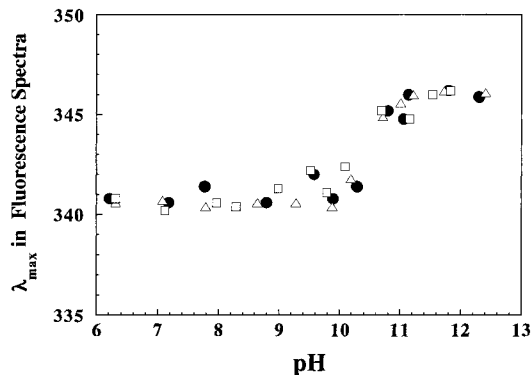


Figure 7. λ_{\max} of Trp fluorescence for 0.2 g/L lysozyme as a function of pH in the presence of poly(AMPS) (\bullet), poly(A70/AAm) (Δ), poly(A50/AAm) (\square) in 0.2 M NaCl.

$> 80\%$ of the fluorescence of lysozyme,³⁶ it is reasonable to expect effective NRET in the complex if Py labels are located near the active site through hydrophobic interaction. The aggregate form of lysozyme may prohibit NRET because a large number of Trp residues would be buried inside, and subsequently only a small fraction of the Py labels would be accessible to the lysozyme active sites. Therefore, the complexation between lysozyme and polyelectrolytes may be described as follows: Lysozyme aggregates are first bound to the polyelectrolyte at pH 12.3; upon further decrease in pH, the bound lysozyme aggregates dissociate on the same polymer near pH 10.5, leading to NRET, as can be seen in Figures 2 and 3. The NRET observed at $\text{pH} < \sim 10.5$ is apparently due to lysozyme dimers bound to the polymer. If this is the case, it is reasonable that the pH for the onset of NRET is a consequence of the aggregate \rightleftharpoons dimer equilibrium independent of the ionic strength and the polymer charge density, as can be deduced from the results in Figures 6 and 7.

QELS. Figure 8 shows histograms for the distribution of the apparent hydrodynamic diameters of free lysozyme, free poly(A99.5/Py0.5), and a lysozyme-poly(A99.5/Py0.5) mixture measured by QELS at pH 11.5 in 0.2 M NaCl. Lysozyme shows a size distribution with a peak at ~ 10 nm, which corresponds to the lysozyme aggregates, and the polymer shows a broader distribution peaking at ~ 17 nm. The lysozyme-poly(A99.5/Py0.5) mixture shows a peak at ~ 12 nm, which may arise from free constituents and complexes of the lysozyme aggregates with the polymer.

Kokufuta et al.¹⁵ investigated the complexation of various proteins and potassium poly(vinyl alcohol)sulfate without added salt at a constant pH by turbidimetry, QELS, and ELS. They observed that a hydrodynamic diameter for a "primary" complex (i.e., a complex of a number of proteins per single polymer chain) was comparable to the polymer diameter. However, because the primary complexes in the Kokufuta's system were neutral (confirmed by ELS), the primary complexes were subsequently associated with each other to form neutral aggregates (AG1), whose diameters were on the order of 100 nm. In the presence of excess polymers, AG1 further aggregates to form "higher-order aggregates" (AG2) with a diameter near $2 \mu\text{m}$.¹⁵

Figure 9 shows histograms for the size distributions for the lysozyme-poly(A99.5/Py0.5) mixture at varying pHs. At $\text{pH} \geq 11.0$, the size distribution is monomodal with a peak at ~ 12 nm. At this pH, the positive charge on

(36) Imoto, T.; Forster, L. S.; Rupley, J. A.; Tanaka, F. *Proc. Nat. Acad. Sci. USA* **1971**, *69*, 1151.

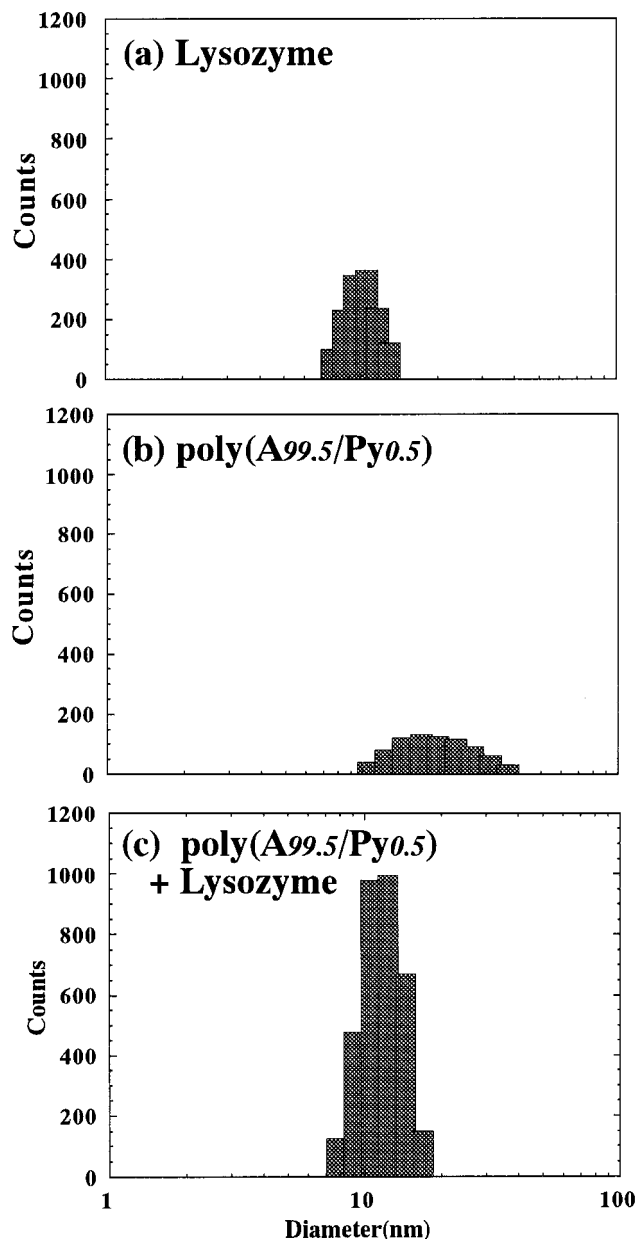


Figure 8. Distribution of apparent diameters for free lysozyme (a), free poly(A99.5/Py0.5) (b), and a lysozyme–poly(A99.5/Py0.5) mixture (c) in 0.2 M NaCl at pH 11.5.

lysozyme is insufficient in magnitude to neutralize the polyanion charge and extensive interpolymer association is prohibited. However, at $\text{pH} \leq 10.5$, particles with much larger sizes are formed, which may correspond to Kokufuta's AG1 and AG2. Unlike Kokufuta's case (without added salt),¹⁵ particles with a mean diameter of ~ 12 nm still exist at $\text{pH} \leq 10.5$, together with the much larger particles.

To confirm that the particles with a ~ 12 -nm diameter are precursors for the larger particles, we measured QELS for lysozyme–poly(A99.5/Py0.5) solutions at $\text{pH} \leq 10.5$ before and after the solutions were filtered with a $0.1\text{-}\mu\text{m}$ syringe filter. We found that the larger particles were detected by QELS even after the solutions were filtered. Because it takes time to obtain an autocorrelated decay function in QELS measurements, we monitored a change in the turbidity ($100 - \%T$ at 420 nm) of a lysozyme–poly(A99.5/Py0.5) solution as a function of time immediately after the solution was filtered with the $0.1\text{-}\mu\text{m}$ syringe filter. Figure 10 shows a change in the turbidity of the

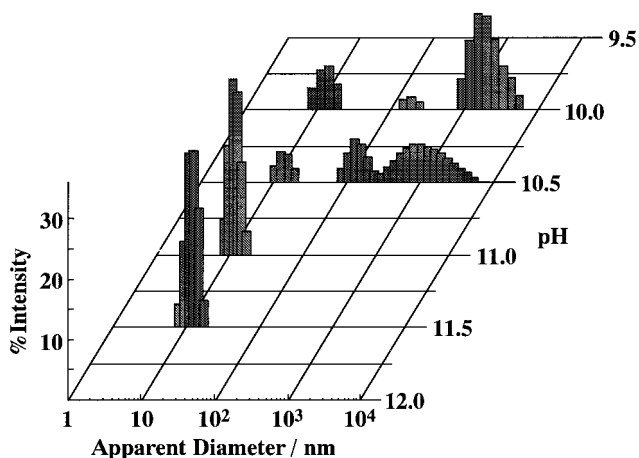


Figure 9. Distribution of apparent diameters for a lysozyme–poly(A99.5/Py0.5) mixture in 0.2 M NaCl at varying pHs.

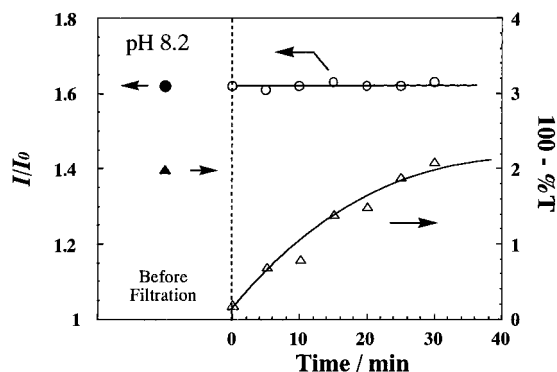


Figure 10. Changes in I/I_0 (○) and turbidity (△) with time for a filtrate of an equilibrated lysozyme–poly(A99.5/Py0.5) solution in 0.2 M NaCl at pH 8.2. I/I_0 and turbidity were monitored as a function of time immediately after the solution was filtered with a $0.1\text{-}\mu\text{m}$ syringe filter. I/I_0 (●) and turbidity (▲) values before filtration are indicated for reference.

solution in 0.2 M NaCl at pH 8.2 with time after filtration. The filtrate was optically clear immediately after filtration. However, the turbidity gradually increased with time. Thus, we conclude that the larger particles are formed from the association of the 12-nm particles and that this association process is in equilibrium. An important observation is that the I/I_0 ratio does not change before and after filtration (Figure 10). The magnitude of NRET immediately after filtration (i.e., the larger particles with diameters $> \sim 100$ nm are eliminated) was the same as that before filtration. Therefore, we can conclude that the 12-nm particles at $\text{pH} \leq 10.5$ (Figure 9) are the primary complexes that are responsible for the NRET and that the larger particles are responsible for the turbidity (Figure 2). The primary complex forms its aggregate in equilibrium at $\text{pH} \leq \sim 10.5$, leading eventually to bulk phase separation when pH is further decreased.

Conclusion

A combination of scattering (turbidimetry, QELS, and ELS), potentiometric, and NRET techniques illuminated the mechanism of the binding of lysozyme to Py-labeled homo- and copolymers of AMPS and AAm. Potentiometric titration revealed that lysozyme bound to the Py-labeled polyanion at pH as high as 12.3, at which pH lysozyme forms aggregates. As the solution pH was decreased, NRET commenced to occur near pH 10.5, accompanied by an increase in turbidity. Neither NRET nor an increase

in the turbidity was observed at $\text{pH} > \sim 10.5$. The pH for the onset of NRET and the turbidity was independent of both ionic strength and polymer linear charge density, indicating that this onset phenomenon was not governed by electrostatic interaction. Thus, we conclude that lysozyme is bound to the polyelectrolytes in its aggregate form in the pH regime from 12.3 to 10.5, and that the bound lysozyme aggregates dissociate into dimers on the polymers at $\text{pH} \leq \sim 10.5$, allowing NRET to occur. The complexes of the lysozyme dimers with the polyelectrolytes form aggregates with sizes 10–100 times larger than those

of the free components at $\text{pH} \leq \sim 10.5$, leading eventually to bulk phase separation at lower pH.

Acknowledgment. The assistance of Shun Edwards at Eli Lilly Corp. in electrophoretic light scattering measurements is acknowledged. This work was supported in part by a Grant-in-Aid for Scientific Research on Priority Areas, "New Polymers and Their Nano-Organized Systems" (No. 277/08246236), from The Ministry of Education, Science, Sports, and Culture, Japan.

LA980366D